Viscoelastic behaviour of gamma irradiated C-S-H

E. Tajuelo Rodriguez, Y. Le Pape
Fusion and Materials for Nuclear Systems Division, Oak Ridge National Laboratory, One Bethel Valley Road, Oak Ridge, TN 37831, USA

W. A. Hunnicutt, P. Mondal
Department of Civil and Environmental Engineering, University of Illinois at Urbana-Champaign, Urbana, IL 61801, USA

ABSTRACT

The license renewal plan of light water reactors in the US to a potential period of 80 years of operation has raised some questions on the effects of radiation in concrete. Cement paste dehydrates due to radiolysis as a consequence of exposure to gamma rays [1]. C-S-H is the main component of cement paste, responsible for its creep properties and it is more viscous with high water content [2]. Drying of C-S-H can cause crosslinking of the silicate chain and a reduction in basal spacing that could potentially impact its viscous behaviour. The viscous response and the Young's modulus of compressed pellets of calcium silicate hydrates with Ca/Si = 0.75, 1 and 1.33, conditioned to 11%RH, were obtained with nanoindentation after gamma doses of 0.39, 0.77 and 1.39 MGy. The morphology, composition and silicate anion structure were studied with TEM, TEM-EDX, XRD and ^{29}Si NMR. Non-irradiated samples were used as control for all experiments. The results show that no significant changes in mechanical properties, morphology or structure are associated to the adsorbed gamma doses.

1. INTRODUCTION

The life cycle of the US fleet of light water nuclear reactors is planned to be extended up to 80 years. After that period, the concrete bio-shield is estimated to withstand high levels of neutron irradiation ($< 5.6 \cdot 10^{19}$ n/cm^2, E > 0.1 MeV [3]) and gamma irradiation (50 to 200 MGy) [3, 4] that could compromise its integrity. Neutrons cause expansion on silicate bearing aggregates [4], while gamma rays cause hydrolysis and hence dehydration of the cement paste [1]. A recent physics-based model has shown that creep delays the onset of damage by neutron irradiation for both restrained and free concrete [5]. This suggests that the viscous behaviour of cement paste plays an important role in mitigating irradiation damage. In that model, creep was considered independent of fluence, but this has not been proved experimentally yet. The literature on creep of gamma-irradiated systems is very scarce, but suggests a reduction of the creep rate [6]. The rates and amplitudes of creep in C-S-H exceed those from other hydration phases and are predominant for the creep response of cement and concrete. The mechanisms for creep in C-S-H are still under debate. The most accepted mechanism is the viscoelastic sliding of particles, blocks or sheets with respect to each other [7-10], although a dissolution-precipitation mechanism induced by stress has also been proposed [11]. A new speculative model of the growth of C-S-H views the movement of a specific type of bond in between C-S-H sheets, involving calcium ions bridging between oxygens in silicate groups, as a possible cause for creep [12]. The stress relaxation of C-S-H depends on its water content: fully saturated specimens present a hydrodynamic component attributed to pore water, while specimens dried to 11% RH and further do not show the hydrodynamic component and their viscous response originates from deformations of the solid body [7]. The partial removal of interlayer water also lowers the stress relaxation in C-S-H [7]. Interlayer water has a more significant structural role for high Ca/Si C-S-H, since the viscous response is more prone to change after drying to 11% or lower RH than for low Ca/Si C-S-H [7]. There are some indications that the viscous response of C-S-H also depends on its chemical structure and its elastic properties [7, 13, 14]. One of the hypothesis is that an increase of Ca/Si ratio and subsequent decrease in both Mean Silicate Chain Length (MCL) and degree of cross-linking (Q^3), would increase the amount of sliding blocks per gram of material to yield a more viscous response, since for instance C_3S pastes cured at high temperatures (more polymerized than at low temperatures) exhibited less creep [15]. C-(A)-S-H was also found to be less viscous than C-S-H, given its longer

aluminosilicate chain length and the presence of cross-linking [14]. Since gamma rays can remove chemically bound water [1] (albeit to a low extent), it is plausible that they can cause a change in viscous behaviour of C-S-H. To verify this hypothesis, synthetic C-S-H of different Ca/Si ratios was gamma-irradiated and post-irradiation examination was carried out for mechanical and chemical properties.

2. MATERIALS AND METHODS

The samples were synthesized by mixing CaO and nanosilica (Aerosil 200) with degassed deionized water at water to solid ratio of 8. The mixtures were milled for 2 days in a tightly sealed 1-L HDPE bottle. The slurries were dried inside a glovebox at 50°C and with a constant N_2 flow of 100cm^3/min for 3 days. The samples were then crushed in an agate mortar and pestle and passed through a 75-µm sieve. The sieved powders were conditioned to 11% RH for 4 weeks. Pellets of 2.54 cm diameter and approximately 2 mm height were pressed at 250 kN in a hydraulic press using 2 g of sample.

The pellets were irradiated in a Co^{60} gamma reactor (J.L. Shepherd Model 109-68 Co-60 unit) to adsorbed doses of 0.39 MGy (2 months), 0.77 MGy (4 months) and 1.39 MGy (7.5 months). The samples were irradiated in stainless steel containers connected to an Ar line and were continuously purged with a gas pressure of 206 kPa (30 psi), to prevent carbonation. Control samples were placed in identical containers connected to the same Ar line, but out of the irradiation chamber. Pellets just after conditioning to 11% RH were also used as control samples.

Thermogravimetry was performed with an STA 449 F1 Jupiter equipped with Netzsch Proteus 6.1 software. 20-30 mg of each ground pellet were used for the analysis. The weight of the sample was monitored increasing the temperature from 20°C to 1400°C at a rate of 20°C/min. An N_2 flow of 58 ml/min was used. The weight percent of water in the samples was calculated from the total weight loss.

XRD was done with a Bruker D2 PHASER desktop x-ray diffractometer that operates at 30 kV and 10 mA. The scans were performed from 5˚ to 80˚ 2θ, step size of 0.03˚ and time per step of 3 s. The basal spacing was calculated by the position of the basal peak applying the diffraction condition equation.

TEM samples were prepared dispersing the ground powder from the pellets on a copper grid with a carbon film. A JEOL JEM-2100F FEG-S/TEM operating at 200 kV was used to examine the morphology of the samples and perform chemical analysis with EDX. Bright field images were taken at magnifications of 15-20kx and spot size of 1. 25-35 EDX points were taken per sample (Aztec software) at 15kx magnification, spot size 1, beam diameter ~ 200 nm and live time of 50 s. A thickness of 200 nm and a density of 2.8 g/cm^3 were used for EDX quantification.

The chemical environment of Silicon nuclei was studied using ^{29}Si DP MAS NMR spectroscopy (Direct Polarization Magic Angle Spinning Nuclear Magnetic Resonance). The scans were done in a Varian Unity INOVA UI300 spectrometer (7.05T) packing the powders in 4mm rotors. The spectra were acquired at 59.6 MHz, employing a spinning speed of 10 kHz, π/2 tip angle, proton decoupling, and 90 s-relaxation delay. A total of 940 scans were collected. The spectra were deconvoluted using the Mnova (Mestrelab Research) software to obtain the percentages of the silicate connectivities. One frequency was used for Q^1, two frequencies for Q^2 and one frequency for Q^3 when present. The silicate mean chain length (MCL) was calculated with the expression:

$$MCL = \frac{2[\%Q^1 + \%Q^2 + \%Q^3]}{\%Q^1}$$

A Hysitron Triboindenter with a Berkovich tip was used for nanoindentation analysis. Stress relaxation was tested reaching a displacement of 175 nm in 1 s, holding for 2 min and unloading in 1 s. A 10x10 grid of indents with 5-µm spacing was used. The thermal drift was minimized using the piezo automation function of the indenter, and putting the tip in contact with the sample for > 3 hours before testing. The settle time used between indents was 1 min. The approximation to a Heaviside scenario for displacement was chosen because the indentation equation has a very simple solution in this case: the normalized force ($P(t)/P_0$) is equal to the normalized relaxation modulus ($E(t)/E_0$) [16]. The data point with the highest load was used to normalize the force. The curves showing an increment of force with time were removed for the analysis. The rest of the curves were filtered through a criterion and discarded if:

- Drift was > 0.2 nm/s
- Force at 50s > Force at 10s
- Force at 100s > Force at 20s

A bootstrap analysis was performed to yield mean force curves with 95% confidence intervals (CI). The mean curve was fitted with a Prony series. The fit of the mean was done starting with a two terms series and adding terms until the error (difference with the bootstrap mean) was < 0.2%.

The elastic response was tested indenting to a load of 4000 µN in 5 s, holding it for 5 s and unloading in 5 s. A 10x20 grid with 10 µm spacing was used, and a settle time of 1 min between indents. The reduced modulus (E_r) was computed from the unload curves (load vs.

displacement) in the equipment software. Curves with drift > 0.2 nm/s and those with kinks in the loading section were rejected to calculate the Young's modulus E:

$$E = E_r(1 - v^2)$$

Where v is the Poisson ratio (0.2 for C-S-H). The mean E with 95% CI were calculated.

3. RESULTS AND DISCUSSION

The XRD patterns of the samples revealed no significant changes in basal spacing with adsorbed gamma dose. The samples with Ca/Si of 0.75, 1 and 1.33 had basal spacings of approximately 12 Å, 11 Å and 10 Å respectively, and all control and irradiated samples with similar compositions showed similar basal spacings. This indicated that chemically bound water in the interlayer was not removed from the structures at the attained doses. The dimension of the basal spacing suggested a harsh degree of drying according to a compilation in ref. [17] . This agreed with the pre-conditioning to 11% RH, that should leave only a monolayer of adsorbed water and the interlayer water. The contained pellets (irradiated and control) showed weight losses from 0.2 to 2.4%. Since interlayer water was not removed, the weight loss must have originated from the loss of adsorbed water. Thermal analysis yielded water contents in the range of 13-17% and there was no apparent correlation with adsorbed doses.

The morphology of the samples was crumpled foil-like. The samples appear denser than others synthesized through the same route [18]. This may have been a consequence of the compaction process. There were no changes in morphology with irradiation (Fig. 1).

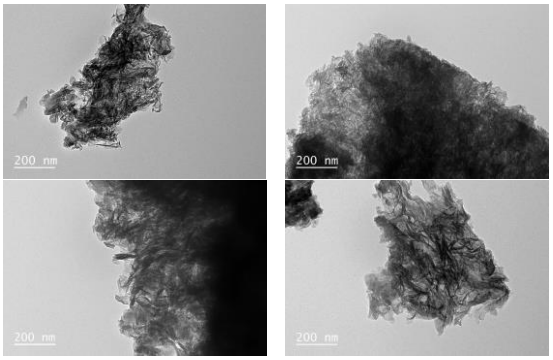

Figure 1. Micrographs of the C-S-H samples with bulk Ca/Si 0.75 (top), 1 (middle). The micrographs on the left column are from the control samples at 11% RH and the ones on the right column belong to the samples irradiated for 4 months.

The normalized force at the end of the hold period showed no correlation with MCL (Fig. 2 bottom), nor the degree of cross-linking (not shown here). The data contradicted the previous hypothesis of a dependence of the normalized force on the mean silicate chain length and/or degree of cross-linking [14]. For a given Ca/Si, there was no dependence of normalized force with adsorbed gamma dose and control and irradiated samples showed comparable normalized forces for a given dose (Fig. 2 top).

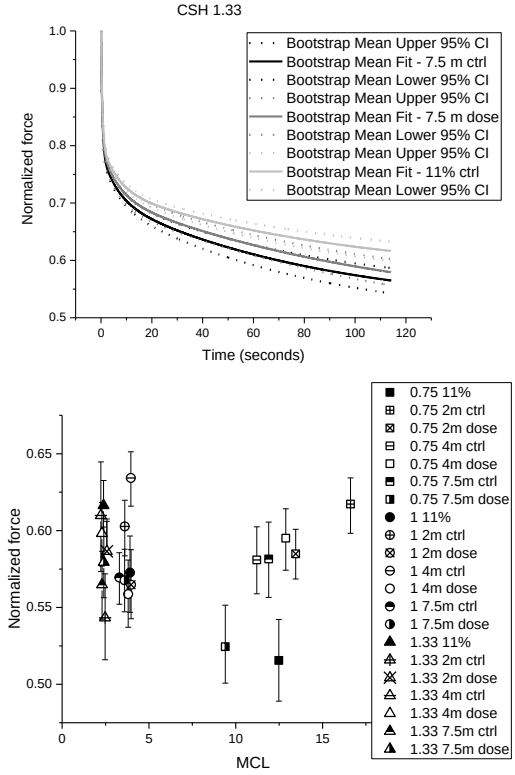

Figure 2. Normalized force over the hold period of stress relaxation tests for samples with bulk Ca/Si 1.33 irradiated for 7.5 months, RH control (11% ctrl) and control from the containers (ctrl) (Top), Normalized force at the end of the hold period vs. mean silicate chain length for all C-S-H samples (gamma-irradiated, control from the containers and control just after conditioning to 11% RH) (Bottom).

The results of Young's modulus did not show any correlation with adsorbed dose for a given Ca/Si. The Young's modulus showed a weak correlation with water weight % (Fig. 3), being higher for higher water content. This agrees with reported hysteresis curves that showed a decrease in Young's modulus with dehydration below 15% RH for cement paste [19].

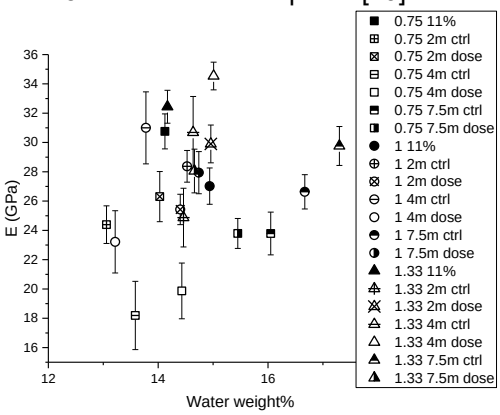

Figure 3. Average Young's modulus for all control and gamma-irradiated C-S-H samples vs. water weight percent.

The average Young's modulus also shows a correlation with average Ca/Si (Fig. 4), being higher for higher Ca/Si. This contradicts predictions from atomic simulations that have shown an increase in Young's modulus with increasing MCL or decreasing Ca/Si [20]. However, there may be other factors such as the porosity of the pellets affecting the average Young's modulus. Therefore, the correlation with Ca/Si may not apply. The increasing density of C-S-H with Ca/Si ratio [17] must had impacted the compaction of the pellets at the same load. In fact, in separate experiments conducted by the second author (Hunnicutt), not reported here, it was found that increasing Ca/Si of the C-S-H produced pellets with lower porosity when compacted under the same pressure, and lower porosity should result in a higher Young's modulus.

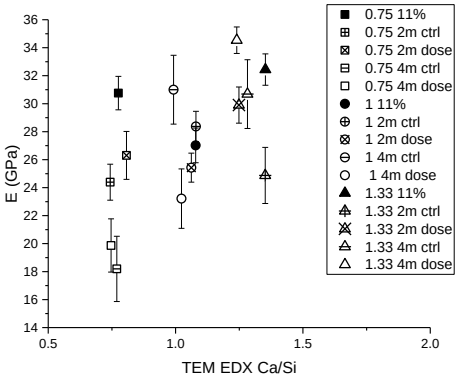

Figure 4. Average Young's modulus for some of the control and gamma-irradiated C-S-H samples vs. average Ca/Si obtained by TEM EDX.

4. CONCLUSIONS

The adsorbed gamma doses of 0.39, 0.77 and 1.39 MGy did not have an impact on the mechanical properties of synthetic C-S-H. The relaxation behaviour and the Young's modulus showed no correlation with gamma dose. The chemical structure (basal spacing, MCL) and water content and morphology showed no variation associated to adsorbed dose. Effects of a dose up to ~ 2 MGy will be studied in the coming months. The use of facilities with higher doses is planned in the future to attain doses of 100-200 MGy, closer to the predicted ones that the concrete bioshield will withstand at the end of the 80 years life cycle in light water reactors.

ACKNOWLEDGEMENTS

This research was sponsored by the U.S. Dep. of Energy, Office of Nuclear Energy, Light Water Reactor Sustainability Program under contract DE-AC05-00OR22725 with UT-Battelle, LLC / Oak Ridge National Laboratory and the U.S. Dep. of Energy Nuclear Science User Facilities for awarded funds through the RTE proposal calls of Sept. 2016 and Jan. 2017.

REFERENCES

[1] Kontani O, Sawada I, Maruyama M, Takizawa M, Sato O, 2013. Evaluation of irradiation effects on concrete structure: Gamma-ray irradiation tests on cement paste, *ASME Power Conference, Amer. Soc. of Mech. Eng.*, pp. V002T007A002-V002T007A002.

[2] Pickett G, 1942. The Effect of Change in Moisture-Content of the Creep of Concrete Under a Sustained Load, *Journ. of the Amer. Concr. Inst.*

[3] Remec I, Rosseel TM, Field KG, Le Pape Y, (2016). Characterization of Radiation Fields in Biological Shields of Nuclear Power Plants for Assessing Concrete Degradation, *EPJ Web of Conferences*, 106:02002.

[4] Field KG, Remec I, Le Pape Y, 2015. Radiation effects in concrete for nuclear power plants–Part I: Quantification of radiation exposure and radiation effects, *Nuc. Eng. and Design*, 282:126-143.

[5] Giorla AB, Le Pape Y, Dunant CF, 2017. Computing creep-damage interactions in irradiated concrete, *Journ. of Nanomech. and Micromech.,* 7:04017001.

[6] McDowall D, 1971. The Effects of Gamma Radiation on the Creep Properties of Concrete, *Proceedings of an Information Exchange Meeting on 'Results of Concrete Irradiation Programmes'*, pp. 55-69.

[7] Alizadeh R, Beaudoin JJ, Raki L, 2010. Viscoelastic nature of calcium silicate hydrate, *Cem. and Concr. Compos.*, 32:369-376.

[8] Tamtsia BT, Beaudoin JJ, 2000. Basic creep of hardened cement paste: A re-examination of the role of water, *Cem. and Concr. Res.*, 30:1465-1475.

[9] Ulm FJ, Le Maou F, Boulay C, 1999. Creep and shrinkage coupling: new review of some evidence, *Revue française de génie civil*, 3:21-37.

[10] Vandamme M, Ulm FJ, 2009. Nanogranular origin of concrete creep, *Proc. of the Nat. Acad. of Sciences*, 106:10552-10557.

[11] Pignatelli I, Kumar A, Alizadeh R, Le Pape Y, Bauchy M, Sant G, 2016. A dissolution-precipitation mechanism explains the origin of concrete creep in moist environments, *Journ. of Chem. Phys*., 145.

[12] Gartner E, Maruyama I, Chen J, 2017. A new model for the C-S-H phase formed during the hydration of Portland cements, *Cem. and Concr. Res.*, 97:95-106.

[13] Alizadeh R, Beaudoin JJ, Raki L, 2011. Mechanical properties of calcium silicate hydrates, *Mat. and Struct.*, 44:13-28.

[14] Hunnicutt WA, Mondal P, Struble LJ, 2016. Effect of Aluminum Substitution in C-S-H on Viscoelastic Properties: Stress Relaxation Nanoindentation, *1st International Conference on Grand Challenges in Construction Materials*.

[15] Bentur A, Milestone NB, Young JF, Mindess S, 1979. Creep and drying shrinkage of calcium silicate pastes IV. Effects of accelerated curing, *Cem. and Concr. Res.*, 9:161-169.

[16] Cao YP, Ji XY, Feng XQ, 2010. Geometry independence of the normalized relaxation functions of viscoelastic materials in indentation, *Philos. Magazine*, 90:1639-1655.

[17] Richardson IG, 2014. Model Structures for C-(A)-S-H(I), *Acta Crystallog. Section B-Struct. Science,* 70:903-923.

[18] Tajuelo Rodriguez E, Richardson IG, Black L, Boehm-Courjault E, Nonat A, Skibsted J, 2015. Composition, silicate anion structure and morphology of calcium silicate hydrates (CSH) synthesised by silica-lime reaction and by controlled hydration of tricalcium silicate (C3S), *Adv. in Appl. Cer.*, 114:362-371.

[19] Feldman RF, Sereda PJ, 1970. A new model for hydrated portland cement and its practical implications, *Engin. Journ.*, 53:53-59.

[20] Manzano H, Dolado JS, Ayuela A, 2009. Elastic properties of the main species present in Portland cement pastes, *Acta Materialia*, 57:1666-1674.